Advance View
https://doi.org/10.3354/meps14368

MARINE ECOLOGY PROGRESS SERIES
Mar Ecol Prog Ser

October 12, 2023

Contribution to the Theme Section 'Small pelagic fish: new research frontiers'

Resolving the variability in habitat use by juvenile small pelagic fish in a major tidal system by continuous echosounder measurements

Margot A. M. Maathuis[1,2,*], Bram Couperus[1], Johan van der Molen[3], Jan Jaap Poos[2], Ingrid Tulp[1], Serdar Sakinan[1]

[1]Wageningen University and Research, Wageningen Marine Research, 1970 AB IJmuiden, The Netherlands
[2]Aquaculture and Fisheries Group, Wageningen University, 6700 AH Wageningen, The Netherlands
[3]NIOZ Royal Netherlands Institute of Sea Research, Department of Coastal Systems, 1790 AB Den Burg (Texel), The Netherlands

ABSTRACT: Shallow coastal areas are important nurseries for larvae and juveniles of many fish species. However, empirical data on small pelagic fish (SPF) in such regions are lacking, and temporal variability in abundance and habitat use by SPF are unknown. Given the critical role of SPF as a trophic link, their commercial value and their sensitivity to climate variability, there is a need for a quantitative and high-resolution monitoring method. We deployed a bottom-mounted echosounder, combined with a water current profiler, to examine the temporal variation in density, vertical distribution and movement behaviour of SPF in the Marsdiep, a dynamic tidal inlet between the North Sea and the Wadden Sea. The acoustic setup provided year-round records of fish density distribution in the water column every 90 min. Monthly fish samples were collected to help interpret acoustic observations. Our analyses indicated that the Marsdiep is a migration gateway for SPF from the North Sea into the Wadden Sea, particularly for juvenile herring and sprat. We observed clear seasonality with high fish densities from mid-spring to early autumn. Fish typically used the upper half of the water column. Swimming behaviour was primarily driven by currents. Yet, during outgoing tide, SPF resisted the outflowing current, suggesting efforts to remain in the Wadden Sea, supporting the hypothesis that the Wadden Sea serves as a preferred nursery area for SPF. Our high frequency, multi-seasonal and vertically resolved observations provide unique insight into the use of the Marsdiep by SPF. Furthermore, potential applications of autonomous echosounder moorings are discussed.

KEY WORDS: Acoustic monitoring · Herring · Small pelagic fish · Sprat · Tidal inlet · Wadden Sea · Wideband autonomous transceiver · WBAT

1. INTRODUCTION

Estuaries and tidal basins around the globe serve as nursery areas for fish (Beck et al. 2001, Baumann et al. 2009), where adult fish either spawn directly, or their larvae drift from further offshore into these areas. Larvae and juvenile fish develop here, and after reaching a certain stage eventually move offshore where they spend the rest of their lives. This pattern also occurs in small pelagic fish (SPF) that provide the trophic link between zooplankton and piscivorous fish, birds and marine mammals. Early life stages of SPF, such as Atlantic herring *Clupea harengus* (hereafter herring) and European sprat *Sprattus sprattus* (hereafter sprat), drift from the North Sea via tidal inlets into the largest intertidal area in the world, the Wadden Sea (Zijlstra 1978, Dickey-Collas et al. 2009, van der Veer et al. 2015,

*Corresponding author: margot.maathuis@wur.nl

Publisher: Inter-Research · www.int-res.com

Couperus et al. 2016). The Wadden Sea is a system of tidal channels and intertidal sand and mud flats, and because of its unique properties, it is listed as a UNESCO World Heritage site. In the Wadden Sea, the biomass of SPF is considered the dominant component of the overall fish biomass; yet, the assemblage of SPF occurring in the Dutch Wadden Sea has hitherto received little research attention (Couperus et al. 2016). We lack empirical data concerning, for instance, SPF quantity, age, growth and temporal migration patterns in this area. Given the central role of SPF in the Wadden Sea ecosystem, insight into the functioning of the food web has so far been limited by this knowledge gap.

Given their short generation times, tight coupling to lower trophic levels, sensitivity to climate variability and aggregation behaviour, SPF populations are known for significant variations in abundance and spatial distribution (Axenrot et al. 2004, Peck et al. 2021). Particularly in the current era of global climate change, where fish populations experience shifts in abundance, distribution and phenology (Rijnsdorp et al. 2009, Sydeman et al. 2015), the variation of occurrence in time and space is increasing even further. Therefore, the study of SPF occurrence and behaviour requires long-term high-resolution acoustic monitoring. However, tidal channels are highly dynamic, and hence complicated to study (Fraser et al. 2017). Yet, the use of hydroacoustic techniques is the only suitable option for long-term continuous monitoring at such sites because high-frequency trawling is impractical and destructive, while use of cameras is impossible due to limited visibility.

Active acoustic techniques are widely used for continuous monitoring (Klemas 2013, Benoit-Bird & Lawson 2016). Recently, the use of bottom-mounted echosounders has become more widespread, for example to explore vertical migration and swimming behaviour of mesopelagic fish (Kaartvedt et al. 2009), to assess the impact of noise on SPF around windfarms (Kok et al. 2021), to study overwintering sprat in a Norwegian fjord (Solberg et al. 2012) and to evaluate if a sparse echosounder mooring array could accurately produce fish abundance indices (De Robertis et al. 2018). In addition, the ecological effects of tidal stream turbines on fish behaviour are often studied using bottom-mounted echosounders (Viehman & Zydlewski 2017, Williamson et al. 2019, Scherelis et al. 2020). Solberg et al. (2012) showed that a bottom-mounted echosounder has several advantages: a stable platform, its non-intrusive nature and its possibilities for long operation times and large data-storage capacity.

Due to the technical challenges imposed by the highly dynamic nature and shallow depth of tidal habitats, knowledge on responses of pelagic fish to dynamic physical conditions is limited. Although most of the Wadden Sea is shallow, with depths typically below 15 m, the inlets between the barrier islands that connect the Wadden Sea to the adjacent North Sea are up to 40 m deep. The largest and westernmost inlet of the Dutch Wadden Sea is the Marsdiep. Herring larvae originating from the English Channel are transported northeast, and a proportion enters the Wadden Sea via this inlet (Dickey-Collas et al. 2009). In addition, tidal inlets are important as feeding areas for predators, as demonstrated by a study of porpoise distribution in the Marsdiep (IJsseldijk et al. 2015). The study showed that porpoise distribution was driven by tidal forces, likely due to the availability of SPF. Therefore, gaining knowledge of SPF behaviour and occurrence as a major food source in the Wadden Sea ecosystem is needed to understand the occurrence and behaviour of their predators. Furthermore, insight in the (timing of) vertical distribution of SPF in the water column is important for understanding feeding patterns and population dynamics of surface-feeding seabirds (Baptist & Leopold 2010, Dänhardt et al. 2011). Moreover, herring and sprat are commercially important species, and their status is assessed annually using indices based on surveys in the North Sea, conducted during specific periods (ICES 2022). However, these seasonally static surveys might not capture phenological changes induced by climate change.

This study is the first to continuously sample fish distribution and current speed in a major inlet into the Wadden Sea for an entire year, using a bottom-mounted autonomous echosounder and a current speed profiler, to better understand SPF density, vertical distribution and movement behaviour. The current speed data from the mooring were supplemented with ferry-borne acoustic Doppler current profiler (ADCP) data of the Marsdiep (van der Molen et al. 2022). Fish density and vertical distribution were investigated for their relation to temporal and environmental variables, including date, time of day, tidal cycle, wind speed, wind direction and lunar cycle. Swimming speed and direction of individual fish were compared to speed and direction of water currents to study fish swimming behaviour and examine how they adapt their direction and speed to the surrounding water currents.

The study had 3 objectives. The first objective was to quantify the temporal variability in fish density in

the Marsdiep during an entire year and examine its relation to environmental factors. Many processes in the life cycle of SPF, for instance spawning and life-stage transitions, are influenced by factors including water temperature and prey abundance (Peck et al. 2013), and therefore are bound to specific time periods. Hence, coastal areas frequently exhibit seasonal utilization patterns by early life stages of fish (Guerreiro et al. 2021). For our study area, it is expected that juvenile SPF drift and migrate towards the coastal zone during spring (Baumann et al. 2009, Dickey-Collas et al. 2009, van Walraven et al. 2017), where they feed and grow, resulting in the highest densities during summer. In autumn, colder Wadden Sea temperatures (van Aken 2008) cause the fish to migrate towards deeper water, resulting in lower abundances during winter. Accordingly, it is expected that seasonality is the most important predictor for SPF density in the Wadden Sea.

The second objective was to investigate the temporal variability in vertical fish distribution. The most critical predictor for vertical fish distribution is expected to be time of day, due to the influence of light intensity on feeding, aggregation behaviour and predator avoidance (Axenrot et al. 2004, Didrikas & Hansson 2009).

The third objective was to study the movement behaviour (i.e. swimming speed and direction) of individual fish in relation to tidal currents. Early life stages of many marine fish are unable to outswim water currents, but there is a significant variation in swimming capacity between species and life stages (Peck et al. 2012). Critical swimming speeds of 0.2–0.9 m s^{-1} have been reported for juvenile herring (Moyano et al. 2016); therefore, we expected that the swimming capacity of SPF is insufficient to outswim the strongest currents in the Marsdiep reaching up to 2 m s^{-1}.

2. MATERIALS AND METHODS

2.1. Study location

Hydroacoustic data were collected in the Marsdiep, the westernmost inlet of the Wadden Sea (Fig. 1). The Marsdiep is a well-mixed tidal inlet with a salinity of around 30 PSU (Buijsman & Ridderinkhof 2007). Here, discharged freshwater from Lake IJssel meets water masses from the North Sea that are moving north-eastward along the Dutch coast. The Marsdiep is about 4 km wide and is the deepest inlet of the Dutch Wadden Sea, with a maximum depth of over 40 m. The Marsdiep seafloor consists of medium-sized sand, with sand dunes several metres high (Buijsman & Ridderinkhof 2007). The tidal currents in this area are strong, reaching a maximum of 2 m s^{-1}, and the average tidal range at Den Helder is approximately 1.4 m. Due to tidal asymmetry, incoming currents are stronger, whereas the duration of outgoing currents is longer (Buijsman & Ridderinkhof 2007).

2.2. Acoustic data collection

Data were collected using a bottom-mounted wideband autonomous transceiver (WBAT) echosounder and an ADCP attached to a stainless-steel frame (Fig. 2). The battery powered Simrad EK80 WBATs were equipped with a 18° split-beam transducer at 38 kHz, and a 7° single beam at 200 kHz. Only the data collected by the 38 kHz transducer were analysed for this study. The Nortek 2 MHz Aquadopp ADCP collected information on water velocity, temperature, azimuth, pitch and roll. Transducers were positioned 0.9 m (i.e. the height of the frame) above the sea floor.

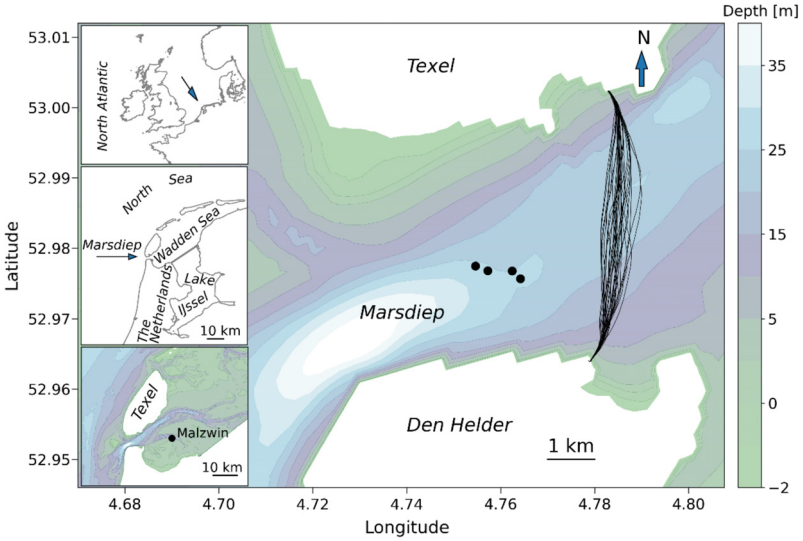

Fig. 1. Study area: Marsdiep—the westernmost tidal inlet of the Wadden Sea located between the island of Texel and the Dutch mainland. Contours depict depths (m) below mean sea level, black dots indicate the wideband autonomous transceiver (WBAT) locations, and black lines depict a selection of ferry crossing trajectories. Insets give an overview of the wider area, zooming in from top to bottom. The black dot labelled 'Malzwin' indicates the stow-net fishing location

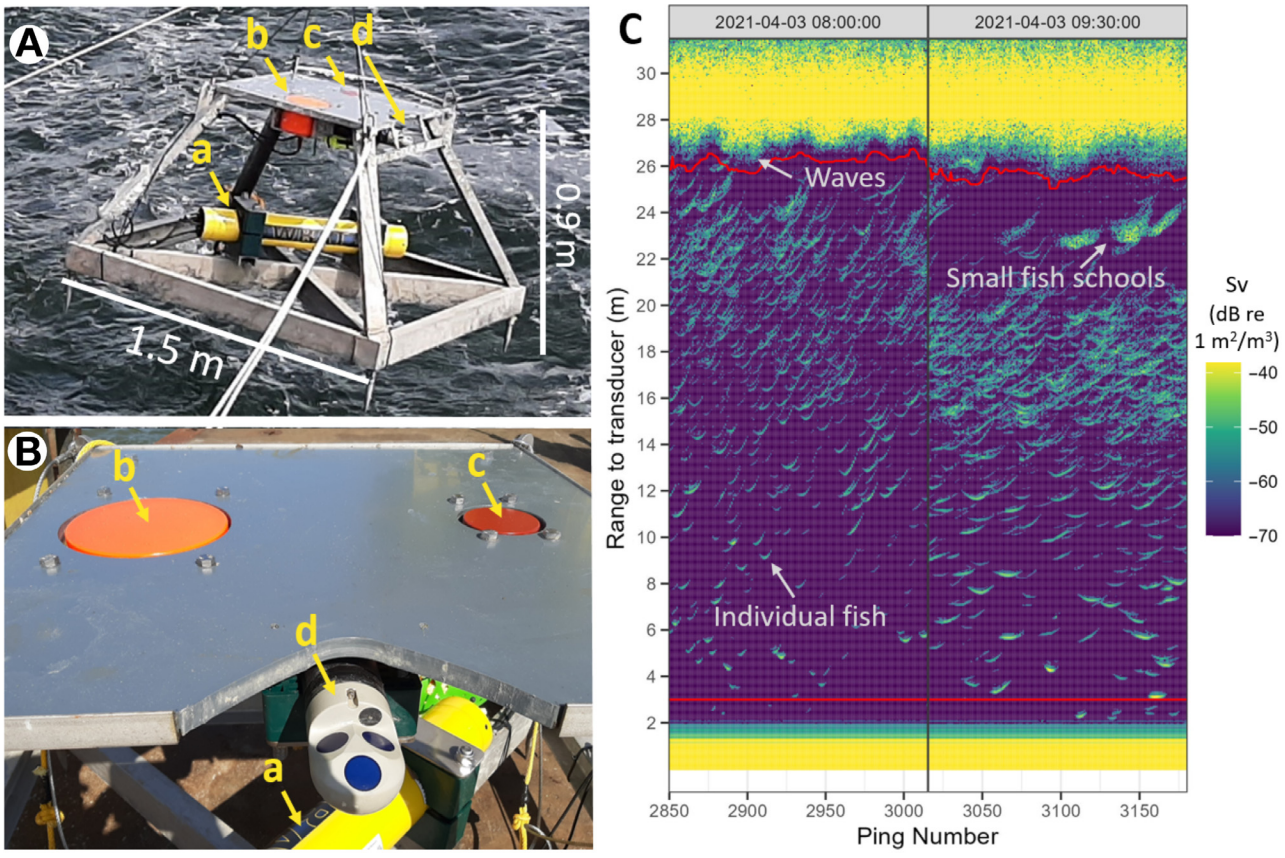

Fig. 2. Acoustic mooring setup shown in (A) side view and (B) top view. The setup includes a WBAT transceiver (a) connected to a 38 kHz split beam (b) and a 200 kHz single beam transducer (c), and an Aquadopp acoustic Doppler current profiler (d). The dimensions of the frame are indicated in white. (C) Echogram of 2 samples taken on 3 April 2021, to illustrate a typical echogram. The *y*-axis represents the range (m) from the transducer, and the *x*-axis represents the ping number. The red lines indicate the bottom and surface exclusion lines, and the colour represents the volume backscatter (S_v in dB re 1 m^2 m^{-3}). The yellow objects between the 2 red lines are recorded traces of fish and fish schools

The total deployment period was 12 mo, ranging from 18 March 2021 until 20 March 2022, with 7 revisits for recovery and deployment operations (see Table S1 in the Supplement at www.int-res.com/articles/suppl/m14368_supp.pdf). All moorings were deployed within 350 m of location 52° 58.60′ N, 4° 45.57′ E, where bottom depth varied between 26 and 29 m. A pilot test was conducted to test the effect of WBAT position on acoustic measurements of fish density, revealing no significant difference in measured backscatter between the locations (for details, see Text S1 and Fig. S1). WBAT calibration was carried out 1.5 mo before deployment, using a 38.1 mm diameter tungsten sphere (Demer et al. 2015); for details, see Table S2.

The WBATs were programmed to transmit pulses of 256 µs in narrowband mode at a ping interval of 0.4 s with a transmission power of 113 W, with the exception of deployments B and C, where a ping interval of 0.25 s was used. Wake-up intervals of 1.5 h were used with 12 'short' (minimum 72 s) and 4 'long' (16 min) measurements per day (referred to as 'sampling interval'). Statistical analysis showed that any short recording would generate the same mean backscatter as the longer recordings (see Text S1 for details).

The ADCP mounted on the frame was programmed to wake up every 10 min to measure current speed and direction. However, it was only able to measure the bottom 10 m of the water column. Therefore, additional ADCP data from a nearby ferry-based time series was used to fill the gaps. This ferry-based ADCP dataset consists of measurements during crossings with 30 min intervals in the Marsdiep each day from 06:00 until 21:00 h using 2 Teledyne RD Instruments Workhorse Monitor 1200 kHz ADCPs mounted at the front and rear of the ferry 4.5 m below the sea surface, and measured at 0.5 m depth intervals. The data of both ADCPs were com-

bined and averaged over 100 latitudinal intervals along each crossing (van der Molen et al. 2022). The sampling locations of the 2 ADCP datasets differed by about 2 km. The frame-mounted ADCP data from March and April 2021 were compared to the ferry ADCP data to evaluate if both produced comparable results. A hydrodynamic model simulation using the model of Duran-Matute et al. (2014) indicated up to 0.2 m s^{-1} faster current speeds at the mooring location in the Marsdiep compared to the ferry crossings, suggesting a need for correction. A conversion factor was derived based on the comparison between the 2 ADCPs over coinciding measurements in depth and time using a least squares fit. Although the ADCP on the ferry recorded data throughout the entire crossing, only a subset of profiles corresponding to a 200 m section at the centre of the inlet was used for this study.

Sea-level height (cm) data were obtained from Rijkswaterstaat from measurements in the Marsdiep relative to the Amsterdam Ordnance Datum (or 'NAP', http://waterinfo.rws.nl). Furthermore, hourly wind speeds and directions for this area were obtained from the Royal Dutch Meteorological Service (KNMI, https://daggegevens.knmi.nl).

2.3. Data collection on fish species composition and size

To help interpret the acoustic observations, fish species composition and fish size distribution were determined during daytime ship-based stow-net fishing in the Marsdiep area at location Malzwin (coordinates: 52° 59.22′ N, 4° 55.29′ E, Fig. 1) once a month in March, May, June, July, September, November and December 2021. Due to bad weather, no samples were taken in April, August and October 2021, and January and February 2022. Stow-net fishing is a passive fishing method using water currents. Hence, sampling was done during highest current speeds at both incoming and outgoing tide. Due to strong winds, only incoming tide was sampled in September and December, and only outgoing tide in November. The average visibility at the sampling location was 0.9 m, the average depth was 5.5 m, and the average sampling duration was 44 min. The net covered the entire water column, and had a stretched mesh size of 20 mm. Although gelatinous organisms were also caught, the focus here was solely on fish, which were measured to the nearest mm. By using a flowmeter (General Oceanics) in front of the net, the catch rate per 1000 m^3 water was calculated.

2.4. Acoustic data processing

Processing and visualisation of acoustic backscatter data was done using Echoview® 13 (Echoview Software). Processing included data calibration, echogram cleaning, individual target detection and tracking. The primary cleaning involved the removal of noise at the surface caused by wind-induced bubbles. The noise boundary was determined by creating lines using 'best bottom candidate' and 'threshold offset' algorithms in Echoview, and further editing these lines manually. Additional sections affected by other noise, such as multiple surface reflections, were masked by manual editing ('bad regions' in Echoview). This procedure was applied to the entire dataset until all significant noise, spikes, ping dropouts and other bad regions were masked. The first 3 m above the transducer were excluded due to transducer nearfield and ringing effects (Simmonds & MacLennan 2005). All manual steps were carried out by the same person twice to ensure consistency. The observed fish data included different kinds of aggregations, such as densely packed small schools, layered shoals with varying depth and density, individual targets and a few large schools. These formations were collectively used to calculate a numerical density indicator: volume backscatter (S_v). The individual targets were further isolated and identified by a tracking algorithm to assess the behavioural patterns and estimate approximate size of individuals. Further data analysis was done using R (version 4.1.0, R Core Team 2021) and RStudio (version 1.3.959; RStudio Team 2020).

2.4.1. Volume backscatter

After cleaning in Echoview, echo integration values were exported using a lower S_v threshold of −65 dB re 1 m^2 m^{-3}. The exported backscatter, as a proxy for SPF density, is considered a quantitative 'ecological unit', rather than being classified into specific species. Jellyfish and ctenophores are present in the area, particularly during summer (van Walraven et al. 2013, 2015). To avoid any influence from their presence on fish density estimates, S_v thresholds were tested ranging from −70 to −50 dB re 1 m^2 m^{-3}. Although stronger thresholds resulted in the removal of more data points, the resulting patterns (e.g. temporal trends and changes in density) remained similar across all tested thresholds, with only changes in the absolute numbers as the threshold became more stringent (Fig. S2). This additional analysis confirmed that the determined threshold of

−65 dB successfully captured the main fish densities while remaining unbiased by noise and untargeted species (such as zooplankton and other gelatinous organisms).

For objective 1, concerning the change in density of fish abundance over time, S_v data collected during each sampling interval were integrated over the water column and treated as 1 sample. For objective 2, concerning the vertical distribution of fish, S_v data were binned into 1 m vertical cells and averaged over each sampling interval. The nautical area scattering coefficient (NASC, Maclennan et al. 2002) was used as an index for fish density. NASC (m^2 nmi^{-2}) represents the integrated backscatter (S_v) from the observed water column scaled to a square nautical mile (n mile) area, commonly used as a proxy for fish density in fisheries acoustic surveys. Although NASC is normally used for describing fish density in studies with a spatial component, it also serves as a standard metric of fish density for stationary studies (De Robertis et al. 2018).

2.4.2. Target tracks

For objective 3, concerning the individual movement of fish, single targets and target tracks were exported including target strength (TS), speed and direction. For single target detection, a TS threshold of −68 dB re 1 m^2 was used (detection settings in Table S3). Prior to track detection, school detection was performed to create polygons, which were used as exclusion masks over the single target echograms to eliminate regions potentially containing overlapping multiple individuals (detection settings in Table S4). Target tracks were detected automatically using the following criteria: a minimum length of 6 pings, including a minimum of 4 data points (i.e. detected single targets), not exceeding a 0.5 m depth difference from ping to ping and containing no more than 3 consecutive empty pings (detection settings in Table S5). These parameters were selected based on series of trial-and-error detections followed by visual inspections. Subsequently, the detected single targets and target tracks were exported for the analysis of fish speed and direction. Occasionally, the algorithm may erroneously identify detections from separate fish as part of the same track, which may result in unrealistic speed estimates. To eliminate such false detections, the tracks were filtered based on an upper fish speed threshold over ground (2.5 m s^{-1}). Estimated speeds faster than this were considered false and were eliminated.

2.5. Data analysis

2.5.1. Fish density and vertical distribution

Two types of models were used to analyse volume backscatter in relation to environmental and temporal variables: generalized additive models (GAMs) for fish density analysis and generalized additive mixed models (GAMMs) for fish vertical distribution analysis. Due to the right-skewed distribution, log-transformed NASC was used as the response variable in the models. The models were constructed using the 'gam' and 'gamm' functions from the 'mgcv' package in R (version 1.8-40, Wood 2017). Data exploration, including outlier detection, assessment of multicollinearity and examination of relationships between NASC and environmental/temporal variables, followed the protocol of Zuur et al. (2010). The models assumed a Gaussian distribution with an identity link function and were visually assessed for meeting the assumptions of homogeneity of variance and normality of residuals.

A GAM was used to determine how much variability in fish density could be explained by nonlinear effects of date, tidal cycle, time of day, temperature, windspeed, wind direction and lunar cycle. Tidal cycle was defined as time (h) after low water slack tide, and lunar cycle was defined as time (h) after full moon; the variance inflation factor confirmed that these 2 variables were not colinear. Because temperature correlated strongly with date, the former was removed from the model. After removing 5% poor-quality observations due to surface exclusion and bad regions, the final dataset comprised 5307 samples to be included in the analysis. Tidal cycle, time of day, wind direction and lunar cycle were included using cyclic cubic regression splines, and date was included using a cubic spline smoother. Windspeed was included as a linear effect. Date and tidal cycle were also included as an interaction term using a tensor spline. We used a basis dimension (k) of 4 for all variables except for date, where we increased k to 7 to capture the strong seasonal variation present in the data. The dredge function in the 'MuMIn' (multimodel inference) package (Bartón 2022) was applied for model selection to determine the order of importance of the explanatory variables based on Akaike's information criterion (AIC, e.g. Burnham & Anderson 2004). Here, explanatory variables were removed from the full model to observe the impact of their removal on model AIC.

A GAMM was used to analyse the vertical distribution of fish density in response to nonlinear

effects of date, time of day and tidal cycle. The water column was divided into samples of 1 m height ('layers'), and since the vertical samples were not independent and multiple samples belonged to the same sampling interval, we used a GAMM with sampling interval as a random effect. After removing 36% poor-quality observations due to surface exclusion and bad regions, the final dataset comprised 78 946 samples to be included in the analysis, corresponding to 3571 sampling intervals. The NASC dataset contained approximately 1.2% zero values; to account for zeros before log-transforming the data, they were replaced by the smallest positive value present, divided by 2. All explanatory variables were added to the model as interactions with depth. The 4 partial effects (depth, date, time of day and tidal cycle) were included individually as well. All interactions were included as tensor smoothing splines, with time of day and tidal cycle included using a cyclic cubic regression spline, and depth and date were included using a cubic spline. No model selection was conducted.

2.5.2. Fish movement relative to tidal currents

Fish speed and swimming direction were compared to current speed and direction to study fish movement behaviour. Fish speed and swimming direction in the horizontal plane were calculated by Echoview based on the range, time and angular position of subsequent targets belonging to the same fish track. Periods of fish tracks that corresponded with available ferry ADCP data were selected. Therefore, the analysis was restricted to daytime (06:00–21:00 h) in the period March until December 2021.

Data were separated into incoming tide (eastward into the Wadden Sea) and outgoing tide (westward into the North Sea). Because we were interested in the differences in fish swimming behaviour between the tidal phases, data from slack tides were removed by excluding periods with low water speeds (<0.5 m s^{-1}).

We aimed to study fish swimming behaviour and examined how fish adapt their direction and speed to surrounding water currents. To quantify swimming effort, fish speed through water was calculated with the following equation:

$$v_{fw} = \mathrm{sign}(v_{fg}) \times (v_{fg} - v_w) \quad (1)$$

where v_{fw} is the fish speed through water, v_{fg} is the fish speed over ground as measured by the echosounder, and v_w is the speed of the water current as measured by the ADCP, all in m s^{-1}. The sign of v_{fg} specifies whether the fish is directed inward (plus) or outward (minus). The multiplication by the direction is added to the formula to scale the outcomes, and to be able to compare the speeds of the 2 tidal phases.

Upon initial examination, we observed that most fish movements were aligned with the mainstream currents in the inlet. To explore how swimming effort was affected by currents, we excluded fish movements in non-mainstream directions based on the frequency of directed swimming at various azimuth angles. Specifically, we eliminated the angles in which fish swam less frequently, i.e. less than the 66$^{\mathrm{th}}$ percentile. Data were binned into 4 m vertical intervals, and we focused on the depth interval 15–19 m, one of the well sampled depth bins. Bins at closer range to the transducer suffered from the low sampling volume where individual fish were less likely tracked (i.e. duration of ensonification in the beam is too short). Conversely, in highly expanded beams farther away from the transducer, multiple targets were more likely to overlap, making it difficult to track individual targets. For the seasonal pattern, we calculated the median fish speed through water per week for both tidal phases.

A total of 1 198 229 target tracks were detected after applying the speed threshold filter. To accurately measure fish speed and exclude jellyfish, we applied a TS threshold. To determine the appropriate threshold value, we estimated fish size using a TS–length equation specific to herring and sprat:

$$\mathrm{TS} = 20\log_{10}(L) - 67.8 \quad (2)$$

where TS is the target strength (dB), and L is the fish length (cm) (Didrikas & Hansson 2004). This allowed us to establish which TS values were associated with fish in our study area. Based on the multiple TS peaks in the fish-tracking dataset, 2 main categories were identified: group 1, consisting of clupeid fish (TS >-60 dB), and group 2, consisting of gelatinous organisms (TS ≤-60 dB). Therefore, we established a TS threshold of -60 dB for the analysis on fish speeds. This TS threshold in combination with the depth bin threshold resulted in a sample size of 194 628 observations for studying fish speed over ground. Furthermore, we obtained current speed data from 6536 ferry crossings, which we used to match with the fish data, resulting in 50 759 samples that enabled us to calculate fish speed through water. In addition, a non-parametric unpaired Wilcoxon rank sum test was performed to determine whether there was a significant difference in the mean fish speed through water between incoming and outgoing currents.

3. RESULTS

3.1. Patterns in fish density and catch data

Fish density in the Marsdiep inlet varied between NASC values of 5 m^2 (n mile)$^{-2}$ to a maximum of around 100 000 m^2 (n mile)$^{-2}$ (Fig. 3). The variation in NASC was particularly high from January 2022 onwards. The observed NASC values increased towards summer, characterized by a first peak around June and a second peak in September, followed by a decline.

The results of the fish catches at location Malzwin in the Marsdiep indicated that Atlantic herring was the dominant SPF, followed by European sprat (Fig. 4A). From March until June, small clupeid post-larvae (i.e. <5 cm) were caught, which could not be identified to species level and were likely a mix of herring, sprat and pilchard. Herring and sprat were present year-round, with a peak of herring in June and July, and a peak of sprat in March. Clupeidae (i.e. the family that includes herring, sprat and pilchard, among others) made up 99% of the catches in the Marsdiep, with herring accounting for 66.7%, sprat for 23.1% and clupeid post-larvae for 9.4%. Other species such as smelt *Osmerus eperlanus*, sand eel (*Ammodytes* spp.), whiting *Merlangius merlangus* and Nilsson's pipefish *Syngnathus rostellatus*, were also observed regularly, although their overall contribution was only approximately 1%. Therefore, the acoustic backscatter, addressed in this study as an SPF ecological unit, mostly represents clupeid species.

The SPF community in the Marsdiep was dominated by small herring and sprat, with overall mean sizes of 6.4

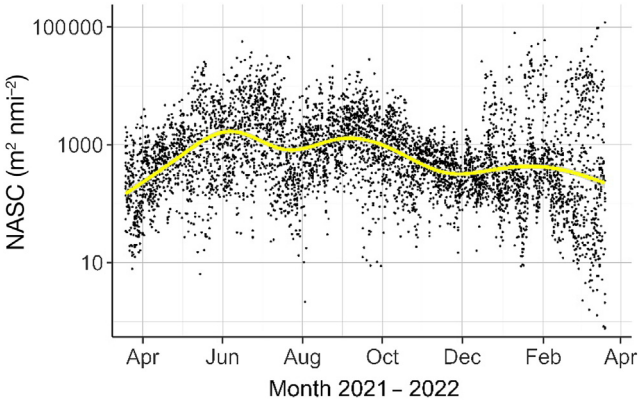

Fig. 3. Fish density values in the Marsdiep over the course of 1 year. Black dots show the observed fish density, presented as nautical area scattering coefficient (NASC, in m^2 nmi^{-2}) on a log scale, and the yellow line shows a generalized additive model smoother

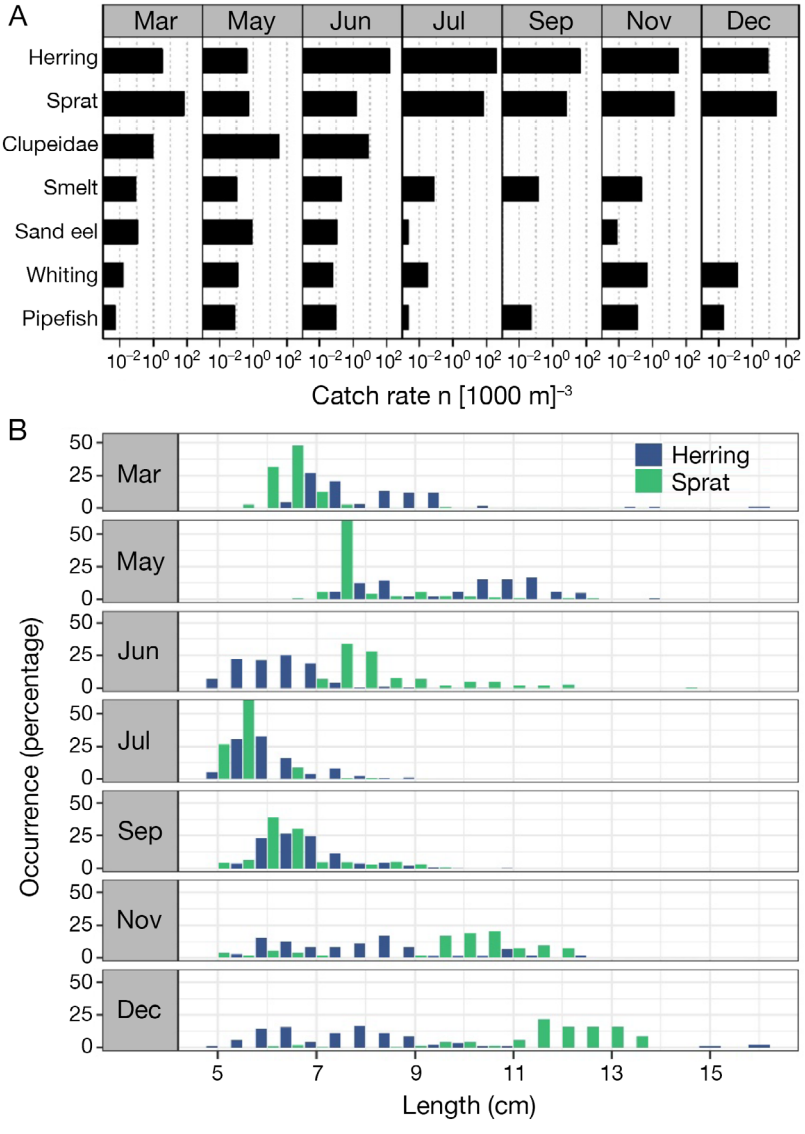

Fig. 4. (A) Fish catch compositions plotted on a log scale; fish are listed in order of decreasing abundance. Scientific names of the species from top to bottom: *Clupea harengus*, *Sprattus sprattus*, unidentified post-larvae (<5 cm) of the family Clupeidae, *Osmerus eperlanus*, *Ammodytes* spp., *Merlangius merlangus* and *Syngnathus rostellatus*. (B) Distribution of size classes (in 0.5 cm intervals, minimum length 5 cm) within the total catch of herring and sprat in the Marsdiep inlet (location Malzwin) from March until December 2021

and 7.3 cm, respectively. The size distributions show seasonal variations, with larger individuals (>10 cm) being primarily observed in May and October for herring, and November and December for sprat (Fig. 4B). In June and July, herring of about 5 cm dominated the distribution, whereas small sprat dominated the distribution in July and September. No clear temporal increase in size was observed, as small individuals (5–6 cm) were consistently present from June until December. In addition to our catch data, the length of SPF was estimated from acoustic data using the TS distribution. The mean TS of detected target tracks from March to December showed 3 distinct peaks (Fig. 5A). The largest peak, at −49.5 dB, corresponds to clupeid fish measuring approximately 8.2 cm (Eq. 2). Additionally, smaller peaks at −57 and −63 dB were observed. The former peak corresponds to clupeid size of about 3.5 cm, while the latter peak is probably dominated by gelatinous organisms. Minimal seasonal variations were observed in the primary TS peak, whereas TS values below −55 dB displayed seasonal variations (Fig. 5B). However, in winter, a different distribution was observed, with the largest peak being −46.5 dB, which corresponds to clupeid fish measuring approximately 11.6 cm.

The GAM, which describes factors affecting the variability in fish density, explained 36.1% of the deviance in the NASC data (Model 1 in Table 1). All variables were significant ($p < 0.001$), highlighting the complexity of the system. Model selection showed that the 2 partial effects of the interaction term could be removed, as the delta AIC was <2. This indicated that most of the information was captured by the interaction of date and tidal cycle, rather than by the factors separately. Subsequently, the first environmental variable to be removed from the model was lunar cycle, resulting in a 40.5 AIC increase. This was followed by wind direction (+43.0), windspeed (+71.3), time of day (+284.9), and finally, the interaction of date and tidal cycle (+792.9). These findings suggest that the interaction of date and tidal cycle was the most influential environmental factor driving fish density in the Marsdiep inlet.

The GAM showed seasonality in fish densities, and mean NASC values depend on the phase of the tidal cycle (Fig. 6). NASC densities at high water slack tide and outgoing tide showed a similar seasonal pattern, with highest NASC values observed around mid-September. For incoming tide and low water slack tide, the peak in NASC was reached around mid-May. In general, highest fish densities were observed from mid-spring until the beginning of autumn. However,

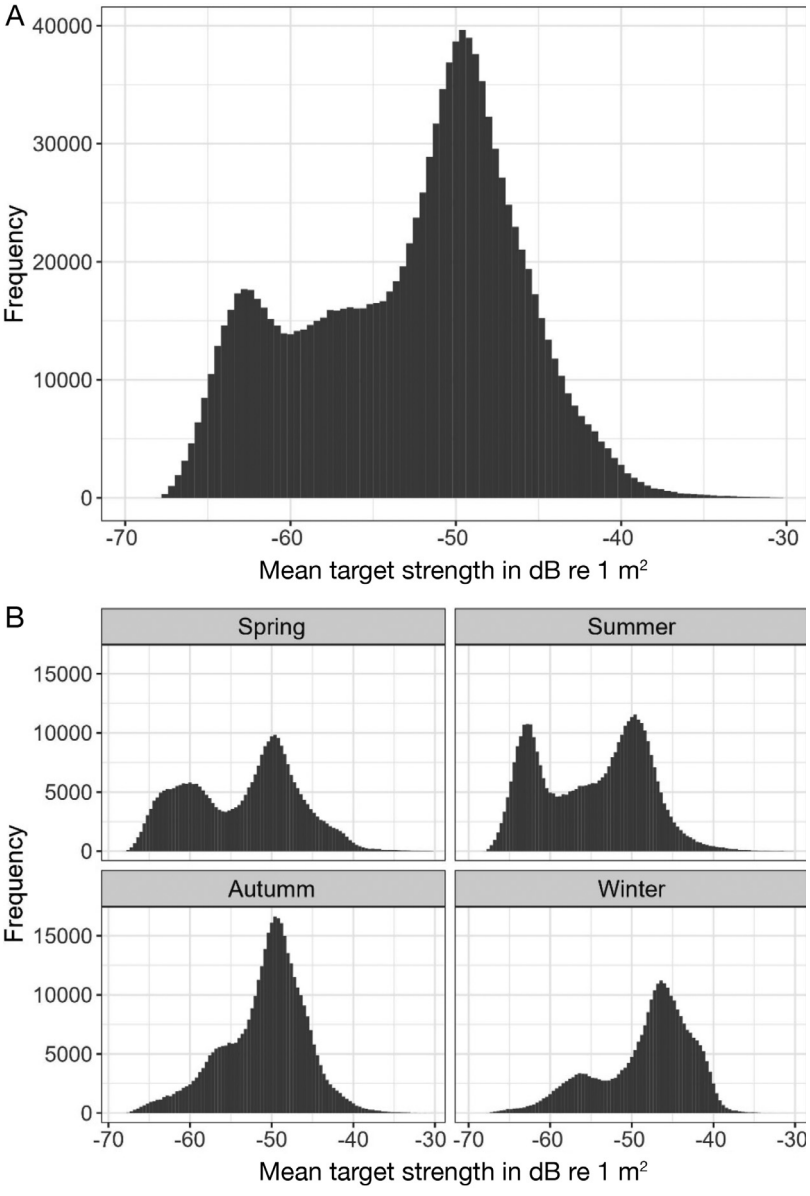

Fig. 5. Mean target strength (dB re 1 m^2) of echo traces in the Marsdiep (A) over the period March until December 2021, corresponding to the dataset utilized for the movement analysis, and (B) over the period March 2021 until March 2022, divided by season

Table 1. Generalized additive model (GAM) and generalized additive mixed model (GAMM) results of the 2 models describing (1) fish density in the total water column and (2) vertical distribution of fish density. EDF: effective degrees of freedom; NASC: nautical area scattering coefficient (m^2 nmi^{-2}); α: intercept; te: tensor product interactions; s: smooth function; *i*: sample; ε: residuals; N: normal distribution; σ standard deviation; β: random effect for sampling interval

Model	Model formula	Type	Terms	EDF	*F*	p
1	$Log(NASC) = \alpha + te(date_i \times tide_i) + s(date_i) + s(tide_i) + s(time_i) + windspeed + s(wind\ direction_i) + s(lunar\ cycle_i) + \varepsilon_i$	GAM	Date × tidal cycle	10.9	72.3	<0.001
			Date	5.9	139.2	<0.001
			Tidal cycle	1.7	6.0	<0.001
			Time	2.0	146.5	<0.001
			Wind speed	−0.006 ± 0.0007[a]		<0.001
	$\varepsilon_i \sim N(0, \sigma^2)$		Wind direction	1.9	22.4	<0.001
			Lunar cycle	1.9	21.3	<0.001
	Full model: 36.1 % deviance explained; intercept 6.7 ± 0.04; $p < 0.001$; $\varepsilon_i \sim N(0, 1.26^2)$					
2	$Log(NASC) = \alpha + s(depth_i) + s(date_i) + s(time_i) + s(tide_i) + te(depth_i \times date_i) + te(depth_i \times time_i) + te(depth_i \times tide_i) + \beta + \varepsilon_i$	GAMM	Depth	3.0	574.6	<0.001
			Date	5.8	109.8	<0.001
			Time	2.0	167.0	<0.001
			Tidal cycle	1.9	12.6	<0.001
	$\beta \sim N(0, \sigma^2_{sampling\ interval})$		Depth × date	14.9	70.3	<0.001
	$\varepsilon_i \sim N(0, \sigma^2)$		Depth × time	8.0	35.6	<0.001
			Depth × tidal cycle	7.6	104.9	<0.001
	Full model: adjusted $R^2 = 0.22$; $\beta \sim N(0, 1.49^2)$; $\varepsilon_i \sim N(0, 1.57^2)$					

[a]As windspeed is included as a non-smoothed linear effect, the values given here represent the estimate of the intercept and the standard error

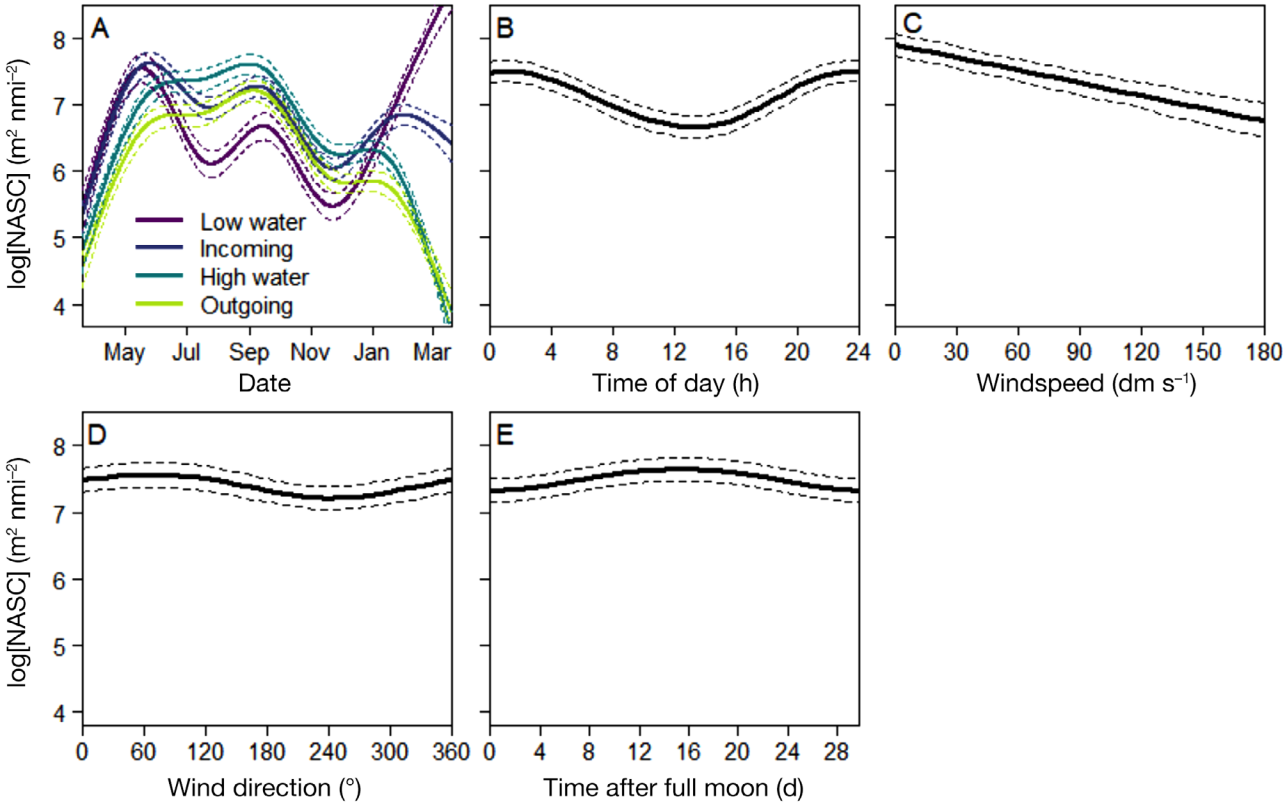

Fig. 6. Generalized additive model for fish density, presented as log-transformed nautical area scattering coefficient (NASC, in m^2 nmi^{-2}). Smoothers for (A) the interaction of date and tidal cycle, (B) time of day, (C) windspeed, (D) wind direction and (E) lunar cycle. The dashed lines present the 95 % confidence intervals, and different colors in (A) indicate the different phases in the tidal cycle: low water slack tide, incoming tide, high water slack tide and outgoing tide. This figure is based on a set of median values used for plotting: time = 00:00 h, date = 20 September 2021, tide = 6 (i.e. high water slack tide), windspeed = 50 dm s^{-1} (Beaufort ~3), wind direction = 220° (SW, dominant wind direction in the Netherlands) and lunar cyle = full moon

at low water slack tide, NASC values increased from December onwards. In addition, fish densities were highest at incoming tide and at high water slack tide for most of the year. Furthermore, densities were lower during daytime, especially around noon. Wind speed and direction both affected fish density, with higher windspeeds resulting in lower NASC values. The highest NASC values were observed for a wind direction of 60°, aligned with the geographical orientation of the Marsdiep. The model showed that the highest NASC values occurred around new moon.

3.2. Vertical distribution

The highest fish densities occurred at depths ranging from 7 to 13 m, with variations across temporal scales such as daily, seasonal and tidal cycles (see Fig. 7 for interactions of temporal variables with depth, and Fig. S3 for partial effects individually). Rather than displaying all months, we depicted a subset of periods: 3 consecutive months in spring (March, April, May), the crucial period for fish-eating birds, and 2 other periods: the beginning of autumn (September) and mid-winter (January). The depth distribution pattern varied by season, with the peak at around 10 m depth being least pronounced in March and most pronounced in January, with intermediate patterns in the other months. Further investigation into the diurnal variation in fish density showed that during the day fish densities were lower towards the surface. At night, fish density was higher compared to daytime, and fish were more evenly distributed up to a depth of about 13 m, after which density declined sharply. Additionally, our results indicate that during outgoing tide fish density was relatively uniform over the water column, whereas during other phases of the tidal cycle there was a clear peak around 10 m.

The GAMM showed that all tested variables had a significant effect ($p < 0.001$) on NASC (Model 2 in Table 1). The adjusted R^2 of the model was 0.22. Validation confirmed that the model assumptions were met, although the replacement of zeroes with half of the observed minimum NASC values created some unwanted patterns in the residuals. The small number of replacements meant that the interpretation of the model was not compromised.

3.3. Individual target tracks: fish movement related to current speed

Current speeds ranged between 0 and 2 m s^{-1} (Fig. 8A). The main current directions were 30° and 210°, representing incoming and outgoing tides, respectively. The absolute fish speed over ground ranged between 0 and 2.5 m s^{-1}, with 1.3 m s^{-1} (4.7 km h^{-1}) being the absolute mean calculated over the full study period (Fig. 8B). The mean directions estimated by the tracked targets aligned well with the main current directions, with an approximate deviation of only 10°, suggesting that the fish orient themselves to the direction of the current flow.

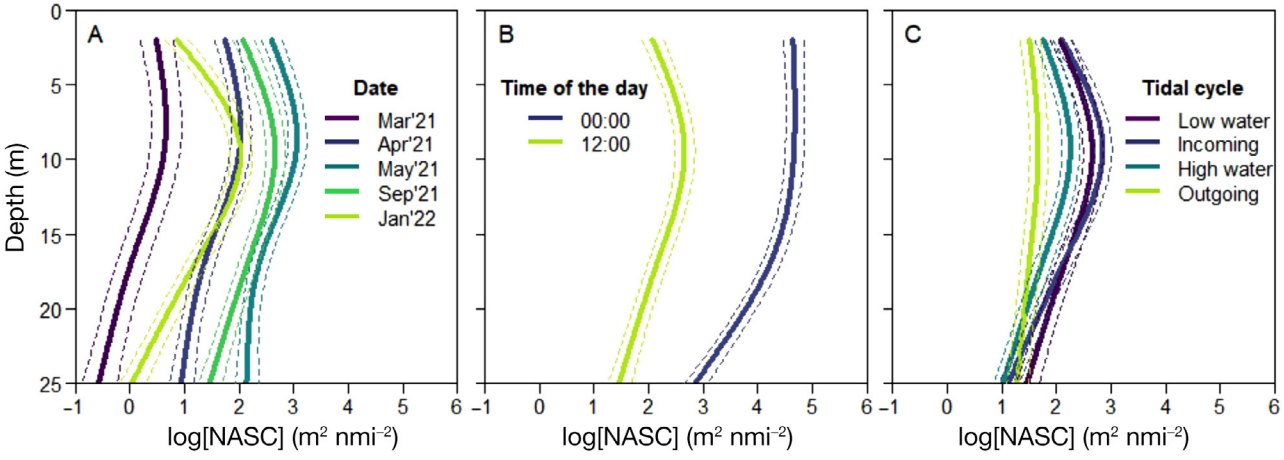

Fig. 7. Generalized additive mixed model showing the vertical distribution of fish, presented as log-transformed NASC (m^2 nmi^{-2}), with depth (m). Smoothers for the interactions of depth with (A) date, (B) time of day and (C) tidal cycle. The dashed lines present the 95% confidence intervals, and different colors indicate different months of the year (A), noon or midnight (B) and phases of the tidal cycle (C). This figure is based on a set of median values used for plotting: time = 12:00 h, date = 20 September 2021, tide = 0 (i.e. low water slack tide). Due to surface interference, there are no data for the upper 2 m. The smoothers of the partial effects can be found in Fig. S3

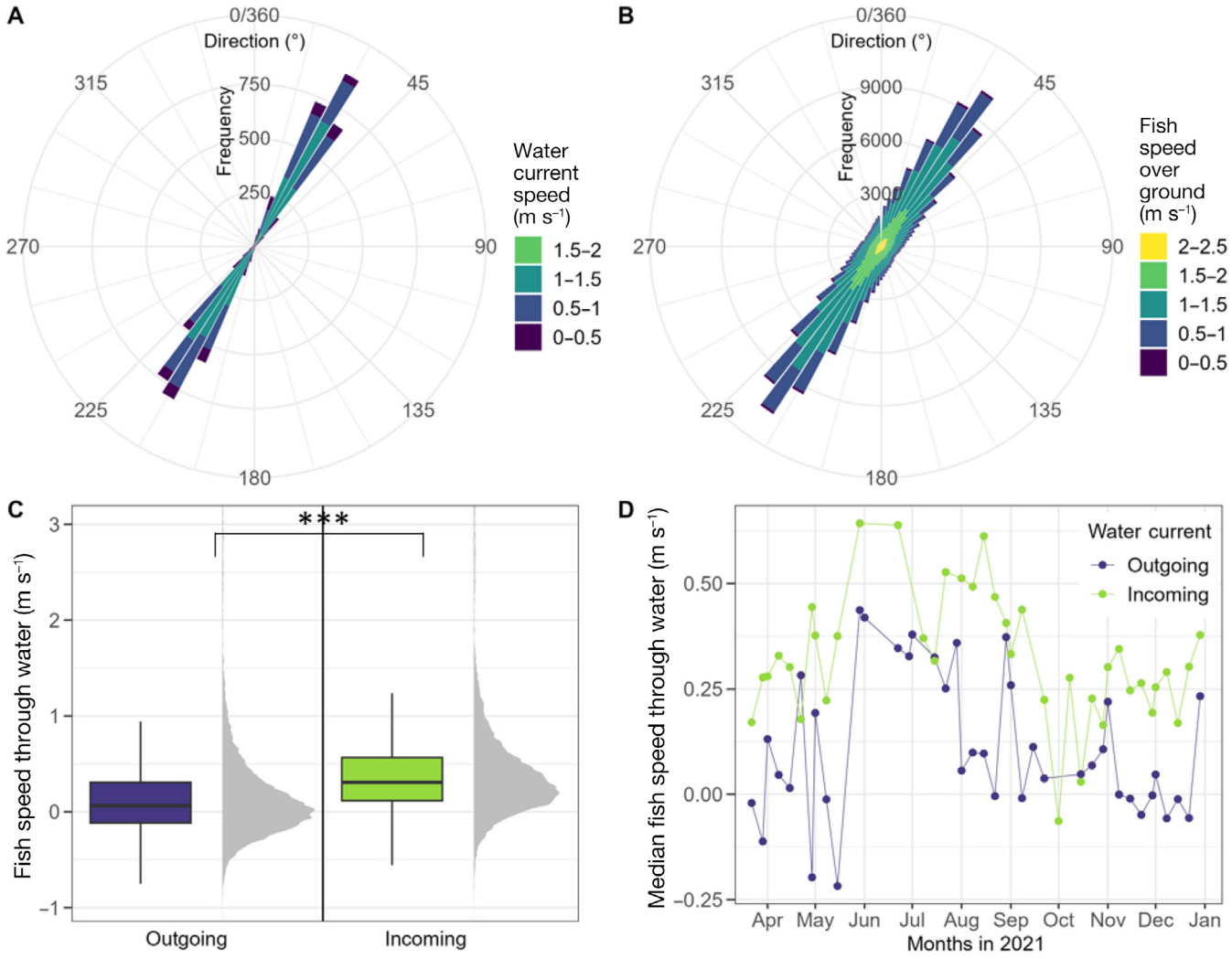

Fig. 8. (A) Water current speed and direction and (B) fish speed over ground and direction. The length of each 'spoke' represents the frequency of directions, and the colours indicate the speed (m s^{-1}). (C) Distribution (boxes show minimum, 1st quartile, median, 3rd quartile and maximum) of fish speed through water (m s^{-1}) at outgoing and incoming tide. Asterisks indicate a significant difference in fish speed through water between outgoing and incoming current (Wilcoxon rank sum test, $W = 117\,961\,711$, $n_1 = 23\,980$, $n_2 = 23\,532$, $p < 0.001$). (D) Median fish speed through water (m s^{-1}) over the season, split between outgoing and incoming tide; only data points that include >100 individual tracks are displayed. Data from March until December 2022 of depths between 15 and 19 m

Fish speed through water revealed swimming behaviour in relation to the current. A positive speed indicated swimming with the current, a zero value indicated swimming against the current to maintain position, and a negative speed indicated movement in the opposite direction of the current. During both tidal phases, fish typically swam with the current and had a positive speed through water (Fig. 8C). Incoming currents resulted in significantly faster fish speeds through water compared to outgoing currents, with means of 0.42 and 0.18 m s^{-1} respectively (W =117961711, n_1 = 23980, n_2 = 23532, $p < 0.001$). Negative fish speeds through water were observed more frequently during outgoing currents. Furthermore, fish speeds through water were highest during summer months (Fig. 8D).

4. DISCUSSION

4.1. Patterns in fish density related to fish catches

The scope of this study was to study temporal variability in SPF density, vertical distribution and movement behaviour in a major tidal inlet of the Wadden Sea. The highest fish densities were observed from

mid-spring until the beginning of autumn. Catch data from location Malzwin suggest that this increase can be attributed to the movement of juvenile herring and sprat from the North Sea into the Wadden Sea. Interestingly, no clear temporal increase in size was observed, which would be expected if a single cohort was present and exhibited growth over time. Furthermore, herring in March and May were larger compared to June and the remainder of the year, when the distribution was dominated by herring measuring 5–6 cm. This suggests that juvenile herring from multiple origins pass through the Marsdiep at different times in the year and that the Marsdiep is a suitable habitat for the small size classes of clupeids.

In the North Sea, 4 large herring spawning components have been described based on their spawning ground and timing. The Orkney-Shetland component spawns first in August/September, followed by the Buchan and Banks component in September/October, and the Downs component spawns latest in December/January (Payne 2010). A modelling study showed that larvae of Downs herring drift from the English Channel north-eastward before arriving in the Wadden Sea after mid-April, although annual variation in timing and abundance is high (Dickey-Collas et al. 2009). The size distribution of herring in the Marsdiep indicated a new year-class entering in June, potentially corresponding to juvenile Downs herring. However, the observed increase in density already started in April, but the size of herring (7–8 cm) was too large to be attributed to juvenile Downs herring (Heath et al. 1997). Hence, this indicates the involvement of another spawning component. Furthermore, the presence of small individuals later in the year suggests the possibility of yet another batch of herring arriving. These individuals do not necessarily have to belong to one of the large components mentioned above, but may belong to smaller coastal stocks, which are known to be present in the whole North-East Atlantic. Hence, it remains unclear which specific herring spawning components use the Wadden Sea for their juvenile stages, necessitating future studies utilizing techniques such as DNA discrimination (Kongsstovu et al. 2022, Bekkevold et al. 2023). Instead of the Wadden Sea being an area where herring of a certain spawning component grow up, the results indicate that it is a suitable area for herring of a certain size range that may originate from different spawning components. Additionally, the increase in NASC can be partly explained by migration of juvenile sprat. Adult sprat have a longer spawning period that typically ranges from March to August, but that can begin as early as January in the English Channel when the temperature threshold of 6°C is reached, and progressively later in more north-eastern areas such as the German Bight (Alshuth 1988, Baumann et al. 2009).

The seasonal fish density pattern was influenced by the phase of the tide. The primary peak around mid-May was mostly driven by high fish densities at low water slack tide and incoming tide. Fish densities were higher at night, similar to Scherelis et al. (2020), which may be due to the presence of larger size classes, nocturnal species (Maes et al. 1999, Didrikas & Hansson 2009) or small-scale migration, both horizontally and vertically.

No other recent studies have conducted year-long, high-temporal-resolution monitoring of pelagic fish in the Wadden Sea. Rademaker et al. (unpubl. data) modelled weekly catches of herring in the Marsdiep during spring and autumn based on fyke observations at the southern tip of Texel to study herring movement into the Wadden Sea. They found that, during the past 39 yr, the time of year was the most important factor affecting herring catches, alongside lunar illumination and relatively low water temperatures in the North Sea. The highest captures were recorded consistently between July and October, which is similar to our findings, although over time there has been a relative increase in catches earlier and a relative decrease in captures later in the year, indicating a small shift in phenology. Also, Couperus et al. (2016) found the highest fish densities at incoming tide during their surveys in May and October in the Marsdiep.

March 2022 recordings showed more extreme fish densities compared to March 2021, suggesting large annual variation. Such variation is expected because herring experience high variability in recruitment (Payne et al. 2009, Burbank et al. 2023), for instance due to interannual variations in year-class strength (Nash & Dickey-Collas 2005) and fluctuations in larval transport resulting from variations in hydrodynamical circumstances (Dickey-Collas et al. 2009). Collecting long-term continuous information on the early life stages of SPF could contribute to fisheries management of herring and sprat in the North Sea. By identifying interannual changes in juvenile abundance and timing, it could provide crucial information on variation in recruitment and year-class strengths, additional to existing indices based on research vessel surveys carried out in specific periods of the year (ICES 2022). Continuous monitoring is especially relevant for capturing changes in the

timing of migration and nursery use. Phenological shifts due to temperature changes have been reported for a wide range of taxa, including fish larvae (Asch 2015) and zooplankton (Heneghan et al. 2023). Experiments on Downs herring demonstrated faster development in warmer waters, and lower fertilization and hatching rates (Toomey et al. 2023). Given the expected increase in sea surface temperature, it is crucial to closely monitor potential shifts in timing to inform fisheries management.

4.2. Patterns in vertical distribution of fish

Our study showed extensive temporal variation in the vertical distribution of fish. We expected that time of day would be the primary driver of vertical fish distribution. That was indeed confirmed, but tidal cycle and seasonality also significantly affected the vertical distribution. Our findings are consistent with those of Williamson et al. (2019), who reported that the tidal cycle has an impact on the vertical distribution of the SPF community in Scotland.

Herring and sprat are known to exhibit diel vertical migration (DVM) in several regions, with individuals schooling at deeper depths during daylight hours, in shallower depths after dawn and before dusk, and becoming more dispersed during darkness (Blaxter & Parrish 1965, Nilsson et al. 2003, Solberg & Kaartvedt 2017, Whitton et al. 2020). However, there are also cases of juvenile herring exhibiting an inverse DVM pattern, where they move to shallower depths to evade predators that follow a DVM pattern (Jensen et al. 2011). Although small schools were frequently observed (see example in Fig. 2), we did not often observe the formation of large schools in this area, which might explain why we did not observe DVM behaviour as clearly as theory describes. Yet, we noticed that the fish tended to swim at greater depths during the day and became more dispersed at night. This observation is in line with results of an acoustic mooring study on pelagic fish in a shallow (±20 m) coastal bay in the Baltic Sea, where the median depth of fish was 10.7 m by day and 4.8 m by night (Didrikas & Hansson 2009). In addition, our findings of highest fish densities between 7 and 13 m are similar to those of a daytime ship-based acoustic survey in the Marsdiep (Couperus et al. 2016). The reason for not observing large schools remains unclear, but it could be attributed to the dynamic environment and high turbidity. Turbidity has a negative effect on prey capture (Ortega et al. 2020), which may reduce the need for fish to hide in vast schools.

Several hypotheses have been proposed to explain the vertical distribution of fish, including food availability, predator avoidance and bioenergetics (Cardinale et al. 2003). In the case of the Marsdiep, the water column is usually vertically well-mixed due to wind and strong tidal currents (Buijsman & Ridderinkhof 2007). Hence, we do not expect food availability, salinity or water temperature to be the main driving factors of vertical fish distribution. Instead, predator avoidance may play a significant role, as fish tend to avoid swimming near the surface to evade diving birds, such as terns (e.g. Sandwich tern *Sterna sandvicensis*: Baptist & Leopold 2010; common terns *S. hirundo*: Dänhardt & Becker 2011) and gulls (e.g. lesser black-backed gull *Larus fuscus*: Baptist et al. 2019). Our findings of lower densities of fish towards the surface during daytime support this hypothesis. Meanwhile, the probability of prey capture by terns is also affected by water transparency (Baptist & Leopold 2010), which was not considered in our analysis. Furthermore, terns and gulls typically dive to relatively shallow depths (e.g. lesser black-backed gulls dive within 0.6 m of the sea surface; Baptist et al. 2019). Unfortunately, our method did not cover the zone specifically relevant for diving seabirds. Therefore, future studies should aim to sample as close to the surface as technically possible and include turbidity as a covariate to better understand the relationship between visual predators and the distribution of SPF.

4.3. SPF use the Marsdiep as a gateway to the Wadden Sea

The direction and speed of currents in the Marsdiep are primarily governed by tides. Currents reach high speeds through the inlet and consequently exert significant control over the movement of fish in the area. Our study showed that fish tended to swim with the current, rather than trying to maintain their geographical location by swimming into the current. This is consistent with our expectation, as swimming against a strong current requires higher energy expenditure and results in a higher metabolic cost. Interestingly, during outgoing tide, fish showed a significantly lower speed through water compared to incoming tide. The high positive fish speeds through water observed during incoming tide probably indicate the migration of juvenile herring and sprat towards the Wadden Sea. Conversely, the lower fish speeds and frequent negative values during outgoing tide suggest that fish resist, and at times swim

against the current, when pushed out of the Wadden Sea. This swimming behaviour may indicate that SPF try to remain within the Wadden Sea because it is a more preferred nursery area than the nearby North Sea. Together with the observation of higher fish densities during incoming tide throughout most of the year, this suggests that the Marsdiep inlet serves as a gateway to the Wadden Sea for SPF.

In the dynamic environment of the Marsdiep, mean fish swimming speeds of 0.42 m s^{-1} during incoming tide and 0.18 m s^{-1} during outgoing tide were observed. These values are slightly higher than those reported for juvenile herring in Himmerfjärden Bay in the Baltic Sea (Sweden), which ranged from 0.1 to 0.26 m s^{-1} (Didrikas & Hansson 2009). The observed higher fish swimming speeds during summer months may likely be attributed to higher water temperatures, which affect the metabolism of cold-blooded fish significantly (Beamish 1978). In addition, it is plausible that changes in fish community, such as species composition and size, resulted in different swimming capabilities, which consequently resulted in seasonally different swimming speeds.

Combining continuous data on fish density and swimming behaviour across tidal phases suggests that SPF mainly immigrate into the Wadden Sea via this inlet. However, to study whether there is indeed a net influx of SPF into the Wadden Sea, the acoustic setup needs to be extended to cover multiple inlets, preferably at different positions within a single inlet as well. A probable hypothesis is that the prevailing north-eastward current in the adjacent North Sea causes SPF to enter the Wadden Sea through the Marsdiep, and exit through the easterly inlets. A WBAT array in multiple inlets is needed for a more comprehensive understanding of SPF migration patterns.

4.4. Study limitations on fish movement behaviour

The analysis on fish movement behaviour focused primarily on daytime observations due to the availability of the ferry ADCP data. Most SPF are visual feeders, so fish swimming speed and direction relative to the currents may differ at night when fish are presumably less active (Didrikas & Hansson 2009). Additionally, during daytime, SPF tend to form schools or swim nearer to each other (Blaxter & Parrish 1965), making it difficult to acoustically detect individual tracks. To prevent false detections in fish aggregations (i.e. consisting of multiple fish), all school-like echo traces were initially masked from the data before using the automatic algorithm to detect single targets and target tracks. This approach ensures the reliability and objectivity of the detected tracks. However, the inability to detect individual tracks within aggregations potentially introduced a bias towards free-swimming objects, which may not provide a representative sample of the entire fish community. Consequently, it was necessary to understand what portion of observed targets could be gelatinous organisms and to subsequently exclude them. Therefore, we classified targets based on the TS distribution and calculated corresponding fish sizes (Eq. 2). Since the swim bladder contributes significantly to the TS, the TS–length equation cannot accurately estimate the size of fish larvae lacking a swim bladder. The peak in the TS distribution at −63 dB is likely caused by jellyfish and ctenophores, and therefore we excluded gelatinous organisms using a TS threshold of −60 dB. The main candidate species for this gelatinous group, as also observed in our stow-net catches, are *Mnemiopsis leidyi*, *Pleurobrachia pileus*, *Aurelia aurita, Cyanea* spp. and *Rhizostoma octopus* (van Walraven et al. 2013, 2015, van Walraven 2016). In absence of reported TS values for these specific species, we assumed their TS values to be in the range of other jellyfish species reported in the literature (Brierley et al. 2004, De Robertis et al. 2018, Yoon et al. 2018).

The dominant length of clupeids in the Marsdiep based on the mean TS was 8.2 cm, which is about 1–2 cm larger than the catch data showed. This variation could be attributed to several factors, including the specific TS–length equation applied, the 11 km distance between the sample locations, the catchability of the net and limited availability of catch samples compared to the continuously available TS samples. However, both catch data and the TS analysis consistently indicated the dominance of small fish in the area without clear size progression over time, and generally larger fish during winter.

The location of the acoustic fish observations by the WBAT and the current measurements by the ferry ADCP were approximately 2 km apart. Although this distance may be negligible on an oceanic scale, it could impact the accuracy of the established relationships due to the dynamic topography of the Wadden Sea and its inlet structure. This analysis comparing the speed and direction of currents with fish movement provides a general overview based on averages of large numbers of observations. However, the approach may have masked finer features. Future studies could investigate fish speed and direction at different phases of

the tidal cycle and at various depths, considering the fluctuation of current speeds caused by shear stress. This could provide insights into whether SPF in the Marsdiep use selective tidal transport (i.e. migrations in synchrony with the tidal cycle, Gibson 2003). Future studies could also consider discriminating between species and sizes, for instance using multiple frequencies (Demer et al. 1999) or physics-based scattering models (Yoon et al. 2021), and incorporating fish tilt and the effect of pressure on swim bladder shape and compression (Gorska & Ona 2001, Ona 2001).

4.5. Use of continuous echosounders in dynamic tidal inlets

We describe the fish density patterns in the Marsdiep based on measurements over a relatively small surface area: the diameter of the WBAT beam at the surface is around 7.5 m. Yet, by conducting a small pilot experiment with 4 WBATs, we showed that although the measured area of 1 echosounder is small, it still provides an accurate signal for a larger area. This finding is in line with a previous study by De Robertis et al. (2018), who found that deploying 3 bottom-mounted echo sounders at the right location can provide an index of abundance comparable to a spatial survey. Unfortunately, our setup did not allow for sampling the bottom 4 m, and due to surface interference and air entrainment, the top 2 m were also absent. This means that if fish were distributed close to the surface or bottom during certain periods, they would not be representatively picked up by our equipment. While acoustic sampling near the surface is technically limited, future studies could incorporate the use of multiple instruments concurrently, both upward and downward looking, to include the bottom portion.

The initial intention of this study was to collect data until June 2022. Unfortunately, the echosounder system became unusable after March 2022, being buried under the sand due to fast-moving sand waves of over 4 m height, illustrating the highly dynamic nature of the area. We recommend using this setup in tidal inlets, but our study indicates that local dynamic circumstances can complicate its implementation, and the exact location and retrieving system (either free standing or moored to e.g. a buoy) should be adjusted to local circumstances. After an initial trial and error phase, this method can be highly cost-effective. While it required a substantial time investment to accumulate the essential experience, both in the field and in the analysis, we see opportunities to automate aspects of the analysis, such as data cleaning. If specific tasks in the process can be automated, this method has the potential to be an efficient option for continuous monitoring, potentially replacing, or at least adding to, costly ship-based surveys.

5. CONCLUSIONS

The Marsdiep is a complex tidal inlet, where multiple factors govern the abiotic circumstances and hence affect fish occurrence. Date, time of day, tidal cycle, wind and lunar cycle were all important factors for explaining the variation in either density or vertical distribution of SPF. Our analyses indicate that the Marsdiep inlet serves as a migration gateway for SPF moving from the North Sea into the Wadden Sea, particularly for juvenile herring and sprat. We observed a clear seasonality with a peak in fish density from mid-spring to early autumn. The presence of small juveniles from June until December suggests that Clupeids from multiple spawning components pass through the Marsdiep at different times in the year. Fish were typically distributed between 7 and 13 m depth during daytime. At night, fish were more evenly distributed up to a depth of 13 m, below which their density declined sharply. Fish swimming behaviour was primarily driven by currents, yet we observed more resistance against the current during outgoing tide. This suggests that fish are trying to remain in the Wadden Sea, supporting the hypothesis that the Wadden Sea serves as nursery area for SPF. Furthermore, we demonstrated that our acoustic mooring setup is effective for collecting high-quality continuous time series data on fish density, vertical distribution and swimming behaviour in dynamic tidal inlets. This study showed that continuous acoustic data on SPF can enhance the understanding of the local ecosystem. Additionally, by identifying densities and conditions of juveniles of commercial species, it could also contribute to fisheries management on a regional scale by detecting (inter)annual changes in juvenile abundance and timing, aiding in the understanding of recruitment variability and year-class strengths.

Acknowledgements. This work was funded by the programme Waddentools-Swimway Waddenzee, with financial contributions from the Waddenfonds, the Ministry of Agriculture, Nature and Food Quality, and the Dutch provinces Noord-Holland, Groningen and Friesland. We gratefully

acknowledge support from the crew of the 'Terschelling', especially Dirk de Boer and Arjen Ponger from Rijkswaterstaat. In addition, we thank Dirk Burggraaf and Hans Verdaat for their field assistance. We thank the reviewers for their valuable contributions to an earlier version of the manuscript.

LITERATURE CITED

Alshuth S (1988) Seasonal variations in length frequency and birthdate distribution of juvenile sprat (*Sprattus sprattus*). ICES CM 1988/H:44. ICES, Copenhagen

Asch RG (2015) Climate change and decadal shifts in the phenology of larval fishes in the California Current ecosystem. Proc Natl Acad Sci USA 112:E4065–E4074

Axenrot T, Didrikas T, Danielsson C, Hansson S (2004) Diel patterns in pelagic fish behaviour and distribution observed from a stationary, bottom-mounted, and upward-facing transducer. ICES J Mar Sci 61:1100–1104

Baptist MJ, Leopold MF (2010) Prey capture success of Sandwich terns *Sterna sandvicensis* varies non-linearly with water transparency. Ibis 152:815–825

Baptist MJ, Van Bemmelen RSA, Leopold MF, De Haan D and others (2019) Self-foraging vs facilitated foraging by lesser black-backed gull (*Larus fuscus*) at the Frisian Front, the Netherlands. Bull Mar Sci 95:29–43

Bartoń K (2022) MuMIn: multi-model inference. R package version 1.47.1. https://CRAN.R-project.org/package=MuMIn

Baumann H, Malzahn AM, Voss R, Temming A (2009) The German Bight (North Sea) is a nursery area for both locally and externally produced sprat juveniles. J Sea Res 61:234–243

Beamish FWH (1978) Swimming capacity. In: Hoar WS, Randall DJ (eds) Fish physiology, Vol VII. Academic Press, New York, NY, p 101–187

Beck MW, Heck KL, Able KW, Childers DL and others (2001) The identification, conservation, and management of estuarine and marine nurseries for fish and invertebrates. BioScience 51:633–641

Bekkevold D, Berg F, Polte P, Bartolino V and others (2023) Mixed-stock analysis of Atlantic herring (*Clupea harengus*): a tool for identifying management units and complex migration dynamics. ICES J Mar Sci 80:173–184

Benoit-Bird KJ, Lawson GL (2016) Ecological insights from pelagic habitats acquired using active acoustic techniques. Annu Rev Mar Sci 8:463–490

Blaxter JHS, Parrish BB (1965) The importance of light in shoaling, avoidance of nets and vertical migration by herring. ICES J Mar Sci 30:40–57

Brierley AS, Axelsen BE, Boyer DC, Lynam CP and others (2004) Single-target echo detections of jellyfish. ICES J Mar Sci 61:383–393

Buijsman MC, Ridderinkhof H (2007) Long-term ferry-ADCP observations of tidal currents in the Marsdiep inlet. J Sea Res 57:237–256

Burbank J, DeJong RA, Turcotte F, Rolland N (2023) Understanding factors influencing Atlantic herring (*Clupea harengus*) recruitment: from egg deposition to juveniles. Fish Oceanogr 32:147–159

Burnham KP, Anderson DR (2004) Multimodel inference: understanding AIC and BIC in model selection. Sociol Methods Res 33:261–304

Cardinale M, Casini M, Arrhenius F, Håkansson N (2003) Diel spatial distribution and feeding activity of herring (*Clupea harengus*) and sprat (*Sprattus sprattus*) in the Baltic Sea. Aquat Living Resour 16:283–292

Couperus B, Gastauer S, Fässler SMM, Tulp I, van der Veer HW, Poos JJ (2016) Abundance and tidal behaviour of pelagic fish in the gateway to the Wadden Sea. J Sea Res 109:42–51

Dänhardt A, Becker PH (2011) Does small-scale vertical distribution of juvenile schooling fish affect prey availability to surface-feeding seabirds in the Wadden Sea? J Sea Res 65:247–255

Dänhardt A, Fresemann T, Becker PH (2011) To eat or to feed? Prey utilization of common terns *Sterna hirundo* in the Wadden Sea. J Ornithol 152:347–357

De Robertis A, Levine R, Wilson CD (2018) Can a bottom-moored echo sounder array provide a survey-comparable index of abundance? Can J Fish Aquat Sci 75: 629–640

Demer DA, Soule MA, Hewitt RP (1999) A multiple-frequency method for potentially improving the accuracy and precision of *in situ* target strength measurements. J Acoust Soc Am 105:2359–2376

Demer DA, Berger L, Bernasconi M, Bethke E and others (2015) Calibration of acoustic instruments. ICES Coop Res Rep 326. ICES, Copenhagen

Dickey-Collas M, Bolle LJ, van Beek JKL, Erftemeijer PLA (2009) Variability in transport of fish eggs and larvae. II. Effects of hydrodynamics on the transport of Downs herring larvae. Mar Ecol Prog Ser 390:183–194

Didrikas T, Hansson S (2004) *In situ* target strength of the Baltic Sea herring and sprat. ICES J Mar Sci 61:378–382

Didrikas T, Hansson S (2009) Effects of light intensity on activity and pelagic dispersion of fish: studies with a seabed-mounted echosounder. ICES J Mar Sci 66: 388–395

Duran-Matute M, Gerkema T, De Boer GJ, Nauw JJ, Gräwe U (2014) Residual circulation and freshwater transport in the Dutch Wadden Sea: a numerical modelling study. Ocean Sci 10:611–632

Fraser S, Nikora V, Williamson BJ, Scott BE (2017) Automatic active acoustic target detection in turbulent aquatic environments. Limnol Oceanogr Methods 15:184–199

Gibson RN (2003) Go with the flow: tidal migration in marine animals. Hydrobiologia 503:153–161

Gorska N, Ona E (2001) Modelling herring target strength pressure dependence in the frequency domain. ICES CM 2001/Q:09. ICES, Copenhagen

Guerreiro MA, Martinho F, Baptista J, Costa F, Pardal MÂ, Primo AL (2021) Function of estuaries and coastal areas as nursery grounds for marine fish early life stages. Mar Environ Res 170:105408

Heath M, Scott B, Bryant AD (1997) Modelling the growth of herring from four different stocks in the North Sea. J Sea Res 38:413–436

Heneghan RF, Everett JD, Blanchard JL, Sykes P, Richardson AJ (2023) Climate-driven zooplankton shifts cause large-scale declines in food quality for fish. Nat Clim Change 13:470–477

ICES (2022) Herring Assessment Working Group for the Area South of 62° N (HAWG). ICES Sci Rep 4:16. ICES, Copenhagen

IJsseldijk LL, Camphuysen KCJ, Nauw JJ, Aarts G (2015) Going with the flow: tidal influence on the occurrence of the harbour porpoise (*Phocoena phocoena*) in the Marsdiep area. Neth J Sea Res 103:129–137

Jensen OP, Hansson S, Didrikas T, Stockwell JD, Hrabik TR, Axenrot T, Kitchell JF (2011) Foraging, bioenergetic and predation constraints on diel vertical migration: field observations and modelling of reverse migration by young-of-the-year herring *Clupea harengus*. J Fish Biol 78:449–465

Kaartvedt S, Røstad A, Klevjer TA, Staby A (2009) Use of bottom-mounted echo sounders in exploring behavior of mesopelagic fishes. Mar Ecol Prog Ser 395:109–118

Klemas V (2013) Fisheries applications of remote sensing: an overview. Fish Res 148:124–136

Kok ACM, Bruil L, Berges B, Sakinan S and others (2021) An echosounder view on the potential effects of impulsive noise pollution on pelagic fish around windfarms in the North Sea. Environ Pollut 290:118063

Kongsstovu S, Mikalsen SO, Homrum E, Jacobsen JA and others (2022) Atlantic herring (*Clupea harengus*) population structure in the Northeast Atlantic Ocean. Fish Res 249:106231

Maclennan DN, Fernandes PG, Dalen J (2002) A consistent approach to definitions and symbols in fisheries acoustics. ICES J Mar Sci 59:365–369

Maes J, Pas J, Taillieu A, Van Damme PA, Ollevier F (1999) Diel changes in the vertical distribution of juvenile fish in the Zeeschelde Estuary. J Fish Biol 54:1329–1333

Moyano M, Illing B, Peschutter P, Huebert KB, Peck MA (2016) Thermal impacts on the growth, development and ontogeny of critical swimming speed in Atlantic herring larvae. Comp Biochem Physiol A Mol Integr Physiol 197: 23–34

Nash RDM, Dickey-Collas M (2005) The influence of life history dynamics and environment on the determination of year class strength in North Sea herring (*Clupea harengus* L.). Fish Oceanogr 14:279–291

Nilsson LAF, Thygesen UH, Lundgren B, Nielsen BF, Nielsen JR, Beyer JE (2003) Vertical migration and dispersion of sprat (*Sprattus sprattus*) and herring (*Clupea harengus*) schools at dusk in the Baltic Sea. Aquat Living Resour 16:317–324

Ona E (2001) Herring tilt angles, measured through target tracking. In: Funk F, Blackburn J, Hay D, Paul AJ, Stephenson R, Toresen R, Witherell D (eds) Herring: expectations for a new millennium. Proceedings of the Symposium 'Herring 2000: Expectations for a New Millennium'. University of Alaska Sea Grant College Program AK-SG-01-04, Fairbanks, AK, p 509–519

Ortega JCG, Figueiredo BRS, da Graça WJ, Agostinho AA, Bini LM (2020) Negative effect of turbidity on prey capture for both visual and non-visual aquatic predators. J Anim Ecol 89:2427–2439

Payne MR (2010) Mind the gaps: a state-space model for analysing the dynamics of North Sea herring spawning components. ICES J Mar Sci 67:1939–1947

Payne MR, Hatfield EMC, Dickey-Collas M, Falkenhaug T and others (2009) Recruitment in a changing environment: the 2000s North Sea herring recruitment failure. ICES J Mar Sci 66:272–277

Peck MA, Huebert KB, Llopiz JK (2012) Intrinsic and extrinsic factors driving match–mismatch dynamics during the early life history of marine fishes. Adv Ecol Res 47:177–302

Peck MA, Reglero P, Takahashi M, Catalán IA (2013) Life cycle ecophysiology of small pelagic fish and climate-driven changes in populations. Prog Oceanogr 116:220–245

Peck MA, Alheit J, Bertrand A, Catalán IA and others (2021) Small pelagic fish in the new millennium: a bottom-up view of global research effort. Prog Oceanogr 191: 102494

R Core Team (2021) R: a language and environment for statistical computing. R Foundation for Statistical Computing, Vienna. https://www.R-project.org/

RStudio Team (2020) RStudio: Integrated development for R. RStudio, Boston, MA. http://www.rstudio.com/

Rijnsdorp AD, Peck MA, Engelhard GH, Möllmann C, Pinnegar JK (2009) Resolving the effect of climate change on fish populations. ICES J Mar Sci 66:1570–1583

Scherelis C, Penesis I, Hemer MA, Cossu R, Wright JT, Guihen D (2020) Investigating biophysical linkages at tidal energy candidate sites; a case study for combining environmental assessment and resource characterisation. Renew Energy 159:399–413

Simmonds J, MacLennan D (2005) Fisheries acoustics. Theory and practice, 2nd edn. Blackwell Publishing, Oxford

Solberg I, Kaartvedt S (2017) The diel vertical migration patterns and individual swimming behavior of overwintering sprat *Sprattus sprattus*. Prog Oceanogr 151:49–61

Solberg I, Klevjer TA, Kaartvedt S (2012) Continuous acoustic studies of overwintering sprat *Sprattus sprattus* reveal flexible behavior. Mar Ecol Prog Ser 464:245–256

Sydeman WJ, Poloczanska E, Reed TE, Thompson SA (2015) Climate change and marine vertebrates. Science 350: 772–777

Toomey L, Giraldo C, Loots C, Mahé K, Marchal P, MacKenzie K (2023) Impact of temperature on Downs herring (*Clupea harengus*) embryonic stages: first insights from an experimental approach. PLOS ONE 18:e0284125

van Aken HM (2008) Variability of the water temperature in the western Wadden Sea on tidal to centennial time scales. J Sea Res 60:227–234

van der Molen J, Groeskamp S, Maas LRM (2022) Imminent reversal of the residual flow through the Marsdiep tidal inlet into the Dutch Wadden Sea based on multiyear ferry-borne acoustic Doppler current profiler (ADCP) observations. Ocean Sci 18:1805–1816

van der Veer HW, Dapper R, Henderson PA, Jung AS, Philippart CJM, Witte JIJ, Zuur AF (2015) Changes over 50 years in fish fauna of a temperate coastal sea: degradation of trophic structure and nursery function. Estuar Coast Shelf Sci 155:156–166

van Walraven L (2016) Flexible filter feeders – the gelatinous zooplankton community in the Netherlands after the invasion of the ctenophore *Mnemiopsis leidyi*. PhD dissertation, University of Groningen

van Walraven L, Langenberg VT, van der Veer HW (2013) Seasonal occurrence of the invasive ctenophore *Mnemiopsis leidyi* in the western Dutch Wadden Sea. J Sea Res 82:86–92

van Walraven L, Langenberg V, Dapper R, Witte JI, Zuur AF, Van Derveer H (2015) Long-term patterns in 50 years of scyphomedusae catches in the western Dutch Wadden Sea in relation to climate change and eutrophication. J Plankton Res 37:151–167

van Walraven L, Dapper R, Nauw JJ, Tulp I, Witte JI, van der Veer HW (2017) Long-term patterns in fish phenology in the western Dutch Wadden Sea in relation to climate change. J Sea Res 127:173–181

Viehman HA, Zydlewski GB (2017) Multi-scale temporal patterns in fish presence in a high-velocity tidal channel. PLoS ONE12:e0176405

Whitton TA, Jackson SE, Hiddink JG, Scoulding B and others (2020) Vertical migrations of fish schools determine

overlap with a mobile tidal stream marine renewable energy device. J Appl Ecol 57:729–741

Williamson B, Fraser S, Williamson L, Nikora V, Scott B (2019) Predictable changes in fish school characteristics due to a tidal turbine support structure. Renew Energy 141:1092–1102

Wood SN (2017) Generalized additive models: an introduction with R, 2nd edn. Chapman and Hall/CRC, Boca Raton, FL

Yoon EA, Hwang DJ, Chae J, Yoon WD, Lee K (2018) Behavior and frequency analysis of *Aurelia aurita* by using *in situ* target strength at a port in southwestern Korea. Ocean Sci 53:53–62

Yoon E, Oh WS, Lee H, Hwang K, Kim DN, Lee K (2021) Comparison of target strength of pacific herring (*Clupea pallasii* Valenciennes, 1847) from *ex situ* measurements and a theoretical model. Water 13:3009

Zijlstra JJ (1978) The function of the Wadden Sea for the members of the fish fauna. In: Dankers N, Wolff WJ, Zijlstra JJ (eds) Fishes and fisheries of the Wadden Sea. Wadden Sea Working Group Report 5, Leiden, p 20–25

Zuur AF, Ieno EN, Elphick CS (2010) A protocol for data exploration to avoid common statistical problems. Methods Ecol Evol 1:3–14

Editorial responsibility: Ignacio A. Catalán (Guest Editor), Esplores, Spain
Reviewed by: P. Polte and 1 anonymous referee

Submitted: April 7, 2023
Accepted: June 28, 2023
Proofs received from author(s): September 26, 2023